Probing lepton flavor violation signal via $\gamma\gamma \to \bar{l}_i l_j$ in the left-right twin Higgs model at the ILC

Guo-Li Liu,* Fei Wang, Kuan Xie, and Xiao-Fei Guo

Department of Physics, Zhengzhou University, Henan, 450001, China

(Received 4 January 2017; published 9 August 2017)

To explain the small neutrino masses, heavy Majorana neutrinos are introduced in the left-right twin Higgs model. The heavy neutrinos—together with the charged scalars and the heavy gauge bosons—may contribute large mixings between the neutrinos and the charged leptons, which may induce some distinct lepton-flavor-violating processes. We check $\bar{\ell}_i \ell_j$ $(i, j = e, \mu, \tau, i \neq j)$ production in $\gamma\gamma$ collisions in the left-right twin Higgs model, and find that the production rates may be large in some specific parameter space. In optimal cases, it is even possible to detect them with reasonable kinematical cuts. We also show that these collisions can effectively constrain the model parameters—such as the Higgs vacuum expectation value, the right-handed neutrino mass, etc.—and may serve as a sensitive probe of this new physics model.

DOI: 10.1103/PhysRevD.96.035005

I. INTRODUCTION

One of the problems of the Standard Model (SM) is that the neutrino oscillation experiments indicate that neutrinos are massive and mix with each other, which manifestly requires new physics beyond the SM [1] since in the SM the neutrino masses—and thus lepton-flavor-violating (LFV) couplings—are missing. However, LFV signals are predicted in many new physics models, such as supersymmetry [2], topcolor-assisted technicolor models [3], little Higgs [4] and Higgs triplet models [5], and the left-right twin Higgs (LRTH) [6] models.

In the LRTH model, to provide an origin for the masses of the leptons and to explain the small neutrino masses, right-handed heavy neutrinos are introduced. These right-handed heavy neutrinos can realize the mixings of the neutrinos with the leptons, which can induce LFV processes at the proposed International Linear Collider (ILC) [7], such as the decay $\mu \to e\gamma$ [8]. In this paper we will discuss $\bar{\ell}_i \ell_j$ $(i, j = e, \mu, \tau, i \neq j)$ production via $\gamma\gamma$ collisions in the LRTH model.

Due to its rather clean environment, the ILC can be an ideal collider to probe new physics. At the ILC, in addition to e^+e^- collisions, one can also realize $\gamma\gamma$ collisions [9] with the photon beams generated by the backward Compton scattering of incident electron and laser beams.

However, $\gamma\gamma$ collisions have two advantages over e^+e^- collisions as probes of LFV interactions [10,11] at the ILC. One is that the process $e^+e^- \to \bar{\ell}_i \ell_j$ occurs only via the s-channel, and the rates are suppressed by the photon propagator and the neutral gauge-boson propagator. On the contrary, the process $\gamma\gamma \to \bar{\ell}_i \ell_j$ is free of this. The other advantage is that it may be difficult to suppress the backgrounds of e^+e^- collisions [10]. Since $\gamma\gamma$ collisions may be free of many SM irreducible backgrounds, the LFV productions in $\gamma\gamma$ collision are suitable for detecting the new physics models.

In this work we will study the LFV processes $\gamma\gamma \to \bar{\ell}_i \ell_j$ $(i \neq j$ and $\ell_i = e, \mu, \tau)$ induced by the gauge bosons $W^\pm$, $W_H^\pm$ and charged scalars $\phi^\pm$ in LRTH models, as well as the heavy neutrinos entering the loop. We find that, due to the existence of the heavy neutrinos, the production in the LRTH model has different properties and rich phenomenology.

This paper is organized as follows. In Sec. II we briefly review the lepton sector of the LRTH model and give the couplings involved in our calculation. In Sec. III, we discuss the contributions from the gauge bosons and the charged scalars. In Sec. IV, based on the preceding discussion, we show the parameter constraints related to the processes. Finally, conclusions are given in Sec. V.

II. THE LEPTON SECTOR OF THE LRTH MODEL AND THE RELEVANT COUPLINGS

In the LRTH model [6,8,12], with the global symmetry $U(4) \times U(4)$, the Higgs field and the twin Higgs in the fundamental representation of each $U(4)$ can be written as $H = (H_L, H_R)$ and $\hat{H} = (\hat{H}_L, \hat{H}_R)$, respectively. After each Higgs develops a vacuum expectation value (VEV),

$$\langle H \rangle = (0, 0, 0, f), \qquad \langle \hat{H} \rangle = (0, 0, 0, \hat{f}), \tag{1}$$

the global symmetry $U(4) \times U(4)$ breaks to $U(3) \times U(3)$, with the gauge group $SU(2)_L \times SU(2)_R \times U(1)_{B-L}$ down to the SM $U(1)_Y$. After the breaking, there are six massive gauge bosons left: the SM Z and $W^\pm$, and extra heavier bosons, Z_H and $W_H^\pm$. There are also eight remaining scalars: one neutral pseudoscalar, ϕ^0, a pair of charged scalars $\phi^\pm$,

*guoliliu@zzu.edu.cn

 © 2017 American Physical Society

the SM physical Higgs h, and a $\mathrm{SU}(2)_L$ twin Higgs doublet $\hat{h} = (\hat{h}_1^+, \hat{h}_2^0)$.

Neutrino oscillations [1] imply that neutrinos are massive, and the LRTH models try to explain the origin of the neutrino masses and mass hierarchy. Three families of doublets $\mathrm{SU}(2)_{L,R}$ are introduced in the LRTH models to provide lepton masses,

$$L_{L\alpha} = -i\begin{pmatrix} \nu_{L\alpha} \\ l_{L\alpha} \end{pmatrix}, \qquad L_{R\alpha} = \begin{pmatrix} \nu_{R\alpha} \\ l_{R\alpha} \end{pmatrix}, \tag{2}$$

where the family index α runs from 1 to 3.

In the same way as the first two generations of quarks, the charged leptons also obtain their masses via nonrenormalizable dimension-five operators, which for the lepton sector can be written as

$$\frac{y_l^{ij}}{\Lambda}(\bar{L}_{Li}H_L)(H_R^\dagger L_{Rj}) + \frac{y_\nu^{ij}}{\Lambda}(\bar{L}_{L,i}\tau_2 H_L^*)(H_R^T \tau_2 L_{Rj}) + \mathrm{H.c.}, \tag{3}$$

which will give rise to lepton Dirac mass terms $y_{\nu,l}^{ij} f^2/\Lambda$, once H_L and H_R acquire VEVs.

However, the Majorana nature of the left- and right-handed neutrinos induces Majorana terms (only the mass section) in dimension-five operators,

$$\frac{c_L}{\Lambda}(\bar{L}_{L\alpha}\tau_2 H_L^\dagger)^2 + \mathrm{H.c.}, \qquad \frac{c_R}{\Lambda}(\bar{L}_{R\alpha}\tau_2 H_R^\dagger)^2 + \mathrm{H.c.} \tag{4}$$

Once $H_L(H_R)$ obtains a VEV, both neutrino chiralities obtain Majorana masses via these operators; however, the smallness of the light neutrino masses cannot be well explained.

Then, if we assume that the twin Higgs $\hat{H}_R$ (which is forbidden to couple to the quarks to prevent the heavy top quark from acquiring a large mass of order $y\hat{f}$) couples to the right-handed neutrinos, one finds that [8]

$$\frac{c_{\hat{H}}}{\Lambda}(\bar{L}_{R\alpha}\tau_2 \hat{H}_R^\dagger)^2 + \mathrm{H.c.}, \tag{5}$$

which will give a contribution to the Majorana mass of the heavy right-handed neutrino, in addition to those of Eq. (4).

After the electroweak symmetry breaking, H_R and $\hat{H}_R$ get VEVs, f and $\hat{f}$, respectively [Eq. (1)]. We can derive the following seesaw mass matrix for the LRTH model in the basis (ν_L,ν_R):

$$\mathcal{M} = \begin{pmatrix} c\frac{v^2}{2\Lambda} & y_\nu \frac{vf}{\sqrt{2}\Lambda} \\ y_\nu^T \frac{vf}{\sqrt{2}\Lambda} & c\frac{f^2}{\Lambda} + c_{\hat{H}}\frac{\hat{f}^2}{\Lambda} \end{pmatrix}. \tag{6}$$

In the one-generation case there are two massive states: a heavy ($\sim\nu_R$) and a light one. For the case that $v < f < \hat{f}$, the masses of the two eigenstates are about $m_{\nu_{\mathrm{heavy}}} \sim c_{\hat{H}}\frac{\hat{f}^2}{\Lambda}$ and $m_{\nu_{\mathrm{light}}} = \frac{cv^2}{2\Lambda}$ [8].

The Lagrangian in Eq. (3) induces neutrino masses and the mixings of different generations of leptons, which may be a source of lepton flavor violation [8].

We also consider the contributions of the heavy gauge boson W_H and the charged scalars $\phi^\pm$. The relevant vertex interactions for these processes are

$$\phi^- \bar{l}\nu_{L,R}\colon\ \frac{i}{f}(m_{l_L,\nu_R}P_L - m_{\nu_L,l_R}P_R)V_H \sim ic_H\frac{\hat{f}^2}{\Lambda f}P_L, \tag{7}$$

$$W_{L,R}^- \bar{l}\nu_{L,R}\colon\ \frac{e}{\sqrt{2}s_w}\gamma_\mu P_{L,R}V_H, \tag{8}$$

where V_H is the mixing matrix of the heavy neutrino and the leptons mediated by the charged scalars and the heavy gauge bosons. The vertices of $\phi^-\bar{l}\nu_{L,R}$ can also be expressed in the coupling constants. $\phi^-\bar{l}\nu_R$, for example, is also written as $ic_H\frac{\hat{f}^2}{\Lambda f}P_L$ if we neglect the charged lepton masses and take $m_{\nu_h} = c_H\hat{f}^2/\Lambda$.

III. CALCULATIONS

A. The distribution functions in $\gamma\gamma$ collisions

For $\gamma\gamma$ collisions at the ILC, the photon beams are generated by the backward Compton scattering of incident electron and laser beams just before the interaction point. The number of events is obtained by convoluting the cross section with the photon beam luminosity distribution, and for the $\gamma\gamma$ collider the number of events is obtained as

$$\begin{aligned} N_{\gamma\gamma\to\bar{\ell}_i\ell_j} &= \int \mathrm{d}\sqrt{s_{\gamma\gamma}}\frac{\mathrm{d}\mathcal{L}_{\gamma\gamma}}{\mathrm{d}\sqrt{s_{\gamma\gamma}}}\hat{\sigma}_{\gamma\gamma\to\bar{\ell}_i\ell_j}(s_{\gamma\gamma}) \\ &\equiv \mathcal{L}_{e^+e^-}\sigma_{\gamma\gamma\to\bar{\ell}_i\ell_j}(s_{e^+e^-}), \end{aligned} \tag{9}$$

where $\mathrm{d}\mathcal{L}_{\gamma\gamma}/\mathrm{d}\sqrt{s_{\gamma\gamma}}$ is the photon beam luminosity distribution and $\sigma_{\gamma\gamma\to\bar{\ell}_i\ell_j}(s_{e^+e^-})$ (with $s_{e^+e^-}$ being the energy squared of the e^+e^- collision) is defined as the effective cross section of $\gamma\gamma\to\bar{\ell}_i\ell_j$. In the optimum case, $\sigma_{\gamma\gamma\to\bar{\ell}_i\ell_j}$ can be written as [13]

$$\begin{aligned} \sigma_{\gamma\gamma\to\bar{\ell}_i\ell_j}(s_{e^+e^-}) &= \int_{\sqrt{a}}^{x_{\max}} 2z\mathrm{d}z\hat{\sigma}_{\gamma\gamma\to\bar{\ell}_i\ell_j}(s_{\gamma\gamma} = z^2 s_{e^+e^-}) \\ &\quad\times \int_{z^2/x_{\max}}^{x_{\max}}\frac{\mathrm{d}x}{x}F_{\gamma/e}(x)F_{\gamma/e}\left(\frac{z^2}{x}\right), \end{aligned} \tag{10}$$

where $F_{\gamma/e}$ denotes the energy spectrum of the backscattered photon for an unpolarized initial electron and laser photon beams given by

$$F_{\gamma/e}(x) = \frac{1}{D(\xi)}\left(1 - x + \frac{1}{1-x} - \frac{4x}{\xi(1-x)} + \frac{4x^2}{\xi^2(1-x)^2}\right). \tag{11}$$

The definitions of the parameters ξ, $D(\xi)$, and $x_{\max}$ can be found in Ref. [13]. In our numerical calculation, we choose $\xi = 4.8$, $D(\xi) = 1.83$, and $x_{\max} = 0.83$.

B. Amplitudes for $\gamma\gamma \to \bar{\ell}_i \ell_j$

Via the coupling in Eq. (7), the Feynman diagrams for the production $\gamma\gamma \to \bar{\ell}_i \ell_j$ mediated by the charged gauge bosons are shown in Fig. 1. The contributions from the charged scalars have similar structures as that from the gauge boson. That is, if the boson lines change into scalar lines in Fig. 1 and Fig. 2, they will become the Feynman diagrams contributed by the charged scalars, which are not shown explicitly.

It can also be seen that we have changed Figs. 1(a)–(e) into Figs. 2(e) and 2(f) via extracting a vertex shown as Figs. 2(a)–(d) [14]. To obtain this, we split the propagator in Fig. 1(c) into two parts:

$$\begin{aligned} M_c &\propto \frac{i}{\not{q} - m_i} i\Sigma(q) \frac{i}{\not{q} - m_j} \\ &= \frac{i(\not{q} + m_i)}{m_j^2 - m_i^2} i\Sigma(q) \frac{i}{\not{q} - m_j} + \frac{i}{\not{q} - m_i} i\Sigma(q) \frac{i(\not{q} + m_j)}{m_i^2 - m_j^2}. \end{aligned} \tag{12}$$

In the right-handed terms of Eq. (12), the first term together with Figs. 1(a) and 1(d), and the second term together with Figs. 1(b) and 1(e) can be collected into a vertex, irrespectively. After this arrangement, the momentum-dependent $\bar{\ell}_i \ell_j \gamma$ vertex can be defined as

$$\begin{aligned} \Gamma'^{\bar{\ell}_i \ell_j \gamma}_{\mu}(p_i, p_j) &= \Gamma^{\bar{\ell}_i \ell_j \gamma}_{\mu}(p_i, p_j) + i\Sigma(p_i) \frac{i(\not{p}_i + m_j)}{m_i^2 - m_j^2} \Gamma^{\bar{l}l'\gamma}_{\mu} \\ &\quad + \Gamma^{\bar{l}l'\gamma}_{\mu} \frac{i(\not{p}_j + m_i)}{m_j^2 - m_i^2} i\Sigma(p_j), \end{aligned} \tag{13}$$

where $\Gamma^{\bar{\ell}_i \ell_j \gamma}_{\mu}$ is the penguin diagram contribution to the total $\bar{\ell}_i \ell_j \gamma$ vertex. Then, the calculation of Figs. 1(e) is equivalent to the calculation of the "tree-level" process depicted in Figs. 2(a) and 2(b), which obviously has a simpler structure.

As for the calculation of the $\bar{\ell}_i \ell_j \gamma$ vertex, we can first give the results from the Lorentz structure. To discuss the contribution of the self-energy diagrams, we take Fig. 2(c) as an example, and the amplitude can be written as

$$\mathcal{M}_c \sim \gamma^\rho \frac{1}{\not{p} - \not{k} - m_{\nu_H}} \gamma_\rho \frac{1}{\not{p}} \gamma^\mu \cdot \bar{\ell}_i \ell_j \epsilon_\mu. \tag{14}$$

The electromagnetic gauge invariance $\partial_\mu \mathcal{M} = 0$ requires that this term vanish, and thus Fig. 2(d) vanishes as well.

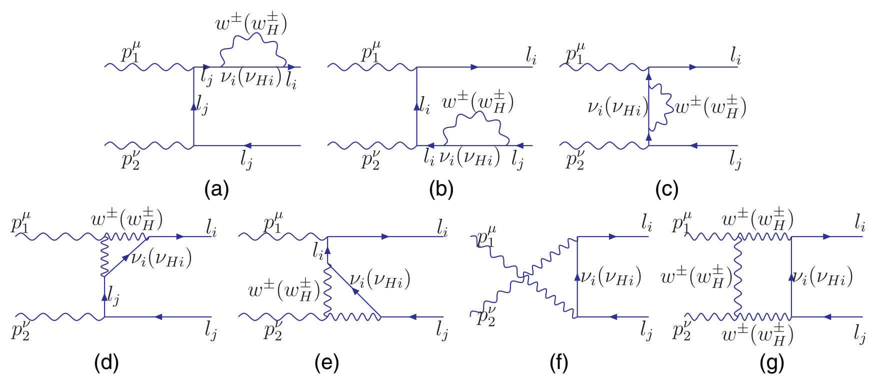

FIG. 1. Feynman diagrams for the production $\gamma\gamma \to \bar{\ell}_i \ell_j$ in the LRTH model mediated by the heavy and light gauge bosons $W^\pm_{L,R}$. Those with two crossed photon lines are not shown.

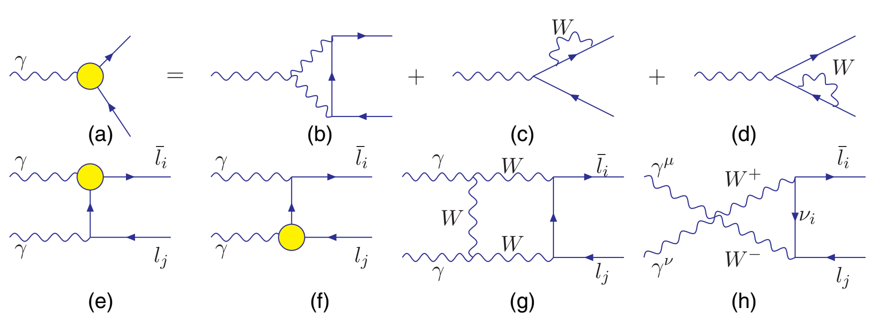

FIG. 2. Feynman diagrams for the production $\gamma\gamma \to \bar{\ell}_i \ell_j$ in the LRTH model, with the triangle and self-energy diagrams replaced by the tree-level vertex (a), i.e., (b), (c), and (d).

So only Fig. 2(b) is left. When we sum over all of the diagrams corresponding to the three intermediate mass eigenstates,

$$\sum_i \left\{ \frac{U^*_{ei} U_{\mu i}}{(p+k)^2 - m^2_{\nu_H}} \right\} = \sum_i U^*_{ei} U_{\mu i} \left\{ \frac{1}{(p+k)^2} + \frac{m_i^2}{[(p+k)^2]^2} + \cdots \right\} = \sum_i \frac{U^*_{ei} U_{\mu i} m^2_{\nu_H}}{[(p+k)^2]^2} + \cdots, \tag{15}$$

the leading term vanishes via the Glashow-Iliopoulos-Maiani mechanism, $\sum_i U^*_{ei} U_{\mu i} = 0$. The second term, with more powers of k in the denominator, has already cleared away the UV divergence.

The penguin contributions from the heavy gauge bosons and the charged scalars in unitary gauge ($\xi \to \infty$)—which are calculated by hand via Feynman parametrization and Wick rotation—can be written as [15]

$$\mathcal{M}_{W_H} = \frac{ce^3}{(\sqrt{2} s_W)^2} \frac{m_i}{64\pi m^4_{W_H}} \bar{u}_i(p)(1-\gamma_5)(2p\cdot\epsilon - m_i \gamma\cdot\epsilon) \times u_j(p-k), \tag{16}$$

$$\mathcal{M}_{H_\pm} = -2e \frac{cm_i}{32\pi f^2 m_H^2} \bar{u}_i(p)(1-\gamma_5)(2p\cdot\epsilon - m_i \gamma\cdot\epsilon) \times u_j(p-k), \tag{17}$$

where $c = \sum_i U^*_{ei} U_{\mu i} m^2_{i\nu_H}$ and $m_{i\nu_H}$ is the ith-generation heavy neutrino mass. p and k are the momenta of the production of the heavier lepton and the photon of the vertex, respectively, and m_i is the heavier lepton mass.

As for the box diagram in Fig. 2(g) and the bosonic quadruple interaction in Fig. 2(h), we have used the calculating tool LoopTools [16].

IV. NUMERICAL RESULTS

In our calculations, we neglect terms proportional to v^2/f^2 in the new gauge boson masses and also in the relevant Feynman rules. We take the SM parameters as [17]

$$m_e = 0.0051\,\text{GeV}, \quad m_\mu = 0.106\,\text{GeV}, \quad m_\tau = 1.777\,\text{GeV},$$
$$m_Z = 91.2\,\text{GeV}, \quad s_W^2 = 0.231, \quad \alpha_e = 1/128.8.$$

However, the internal charged lepton masses m_e, m_μ, and m_τ will be neglected since they are much lighter than the gauge bosons, the charged scalars, and the right-handed neutrinos.

When the gauge boson is mediated in the loop (as shown in Figs. 1 and 2), the relevant parameters are the masses of the gauge bosons m_W, m_{W_H} and the heavy neutrino m_{ν_H}.

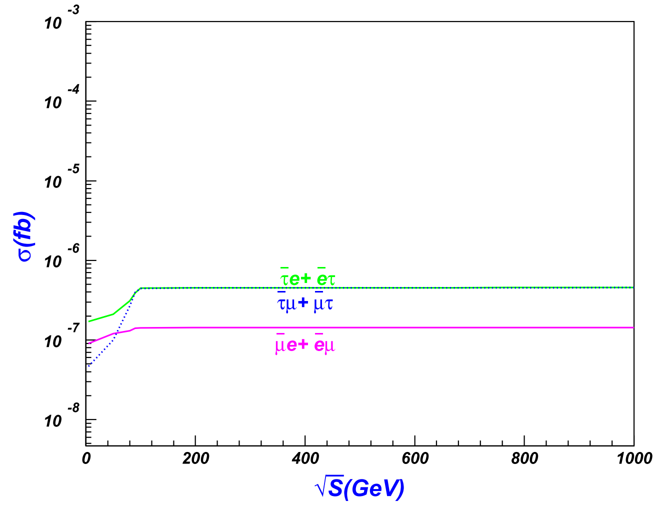

FIG. 3. The cross sections of the processes $\gamma\gamma \to \bar{\mu}e + \bar{e}\mu$, $\to \bar{\mu}e + \bar{e}\mu$, and $\to \bar{\mu}e + \bar{e}\mu$ vary with increasing center-of-mass energy.

On the other hand, the heavy charged bosons may also provide a large contribution to the lepton-flavor-changing processes, which can be realized by replacing the heavy gauge bosons with the charged scalars $\phi^\pm$ in Figs. 1 and 2.

In Higgs-mediated processes, in addition to the masses of the charged scalars m_ϕ and the heavy neutrino m_{ν_H}, the breaking scales f, $\hat{f}$ are also dependent parameters. The light neutrino masses and the charged leptons mixings to the light neutrinos c_i ($\phi^- \bar{l}\nu_{L,R}$) are quite small, so we neglect the contributions mediated by the light neutrinos. We will focus on the heavy neutrinos, whose +++coupling to charged leptons via the charged scalars is proportional to the heavy neutrino mass, i.e., $\sim c_H \frac{\hat{f}^2}{\Lambda f}$.

The masses of the charged scalars and the heavy gauge bosons vary in the ranges $200 \le m_\phi \le 1000$ GeV [18] (sometimes extending to 100 GeV) and $1000 \le M_{W_H} \le 5000$ GeV [19].

Note that in the couplings of $\phi^+(W_H^+)\nu_H^k \bar{\ell}$ there exist the mixing terms V_H^{kl}s, which parametrize the interactions of the charged leptons with the heavy neutrinos (mediated by both $\phi^\pm$ and W_H^+), and they can be chosen as the Maki-Nakagawa-Sakata (MNS) matrix $V_{\rm MNS}$, which diagonalizes the neutrino mass matrix [20,21]:

$$V_{\rm MNS} = \begin{pmatrix} c_{12}c_{13} & s_{12}c_{13} & s_{13}e^{-i\delta} \\ -s_{12}c_{23} - c_{12}s_{23}s_{13}e^{i\delta} & c_{12}c_{23} - s_{12}s_{23}s_{13}e^{i\delta} & s_{23}c_{13} \\ s_{12}s_{23} - c_{12}c_{23}s_{13}e^{i\delta} & -c_{12}s_{23} - s_{12}c_{23}s_{13}e^{i\delta} & c_{23}c_{13} \end{pmatrix}, \tag{18}$$

where $s_{ij} \equiv \sin\theta_{ij}$ and $c_{ij} \equiv \cos\theta_{ij}$. δ is the CP phase.

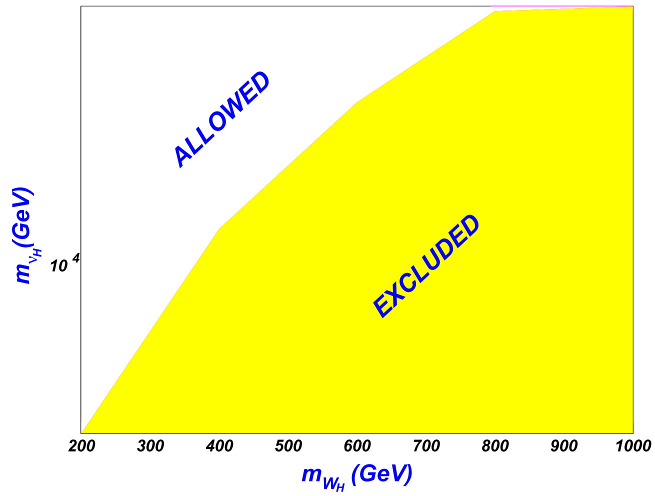

FIG. 4. The contour of the process $\gamma\gamma \to \bar{\mu}e + \bar{e}\mu$, between m_{W_H} and m_{ν_H}.

Three mixing angles θ_{12}, θ_{13}, and θ_{23} can be chosen as free parameters since they are different from those of the SM. The contribution of the CP phase δ, which varies from $0 - 2\pi$, can be a free parameter. But first we take the three mixing angles θ_{12}, θ_{13}, and θ_{23} and the CP phase δ as [22–26]

$$\sin^2 2\theta_{12} \simeq 0.86, \qquad \sin^2 2\theta_{23} \simeq 1,$$
$$\sin^2 2\theta_{13} \simeq 0.089, \qquad \delta \simeq \pi, \tag{19}$$

and in the final discussion we vary them as free parameters.

A. The SM background of the flavor-changing processes

The SM backgrounds of the flavor-changing processes are quite small, since these processes are prohibited at the tree level and are largely suppressed at the one-loop level [27]. The main backgrounds of $\tau\bar{e}$ may be $\gamma\gamma \to \tau^+\tau^- \to \tau\nu_e\bar{\nu}_\tau\bar{e}$, $\gamma\gamma \to W^+W^- \to \tau\nu_\tau\nu_e\bar{e}$, or $\gamma\gamma \to \tau\bar{e}\nu_\tau\nu_e$, which are

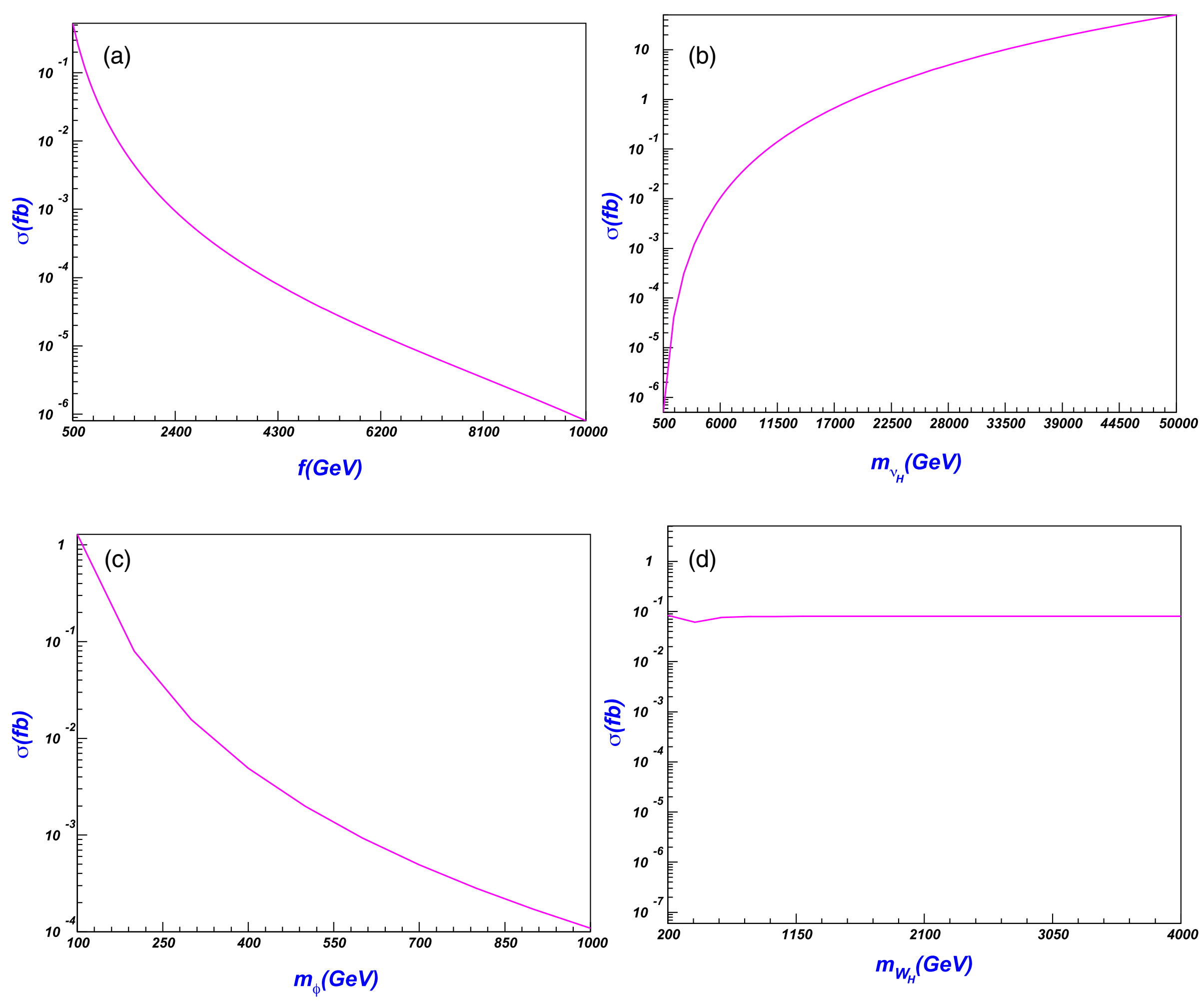

FIG. 5. The cross section σ of the processes $\gamma\gamma \to \bar{\tau}\mu$ as a function of the breaking f, the scalar mass m_ϕ, the heavy neutrino mass m_{ν_H}, and the heavy charged boson mass m_{W_H}, respectively.

suppressed to be 9.7×10^{-4}, 1.0×10^{-1}, and 2.4×10^{-2} fb. If an integrated luminosity of 3.45×10^2 fb^{-1} is chosen for the photon collision [28], the production rates of $\gamma\gamma \to \mu\bar{e}, \tau\bar{e}, \tau\bar{\mu}$ should be larger than 10^{-2} fb to get the 3σ observational significance [27,29].

In the calculation, to avoid the collinear divergence, we require that the scattering angle cut $|\cos\theta_e| < 0.9$ and the transverse momentum cut $p_T^e > 20$ GeV, which are the same as the cuts in Ref. [27]. Therefore, the requirement that the cross section be 10^{-2} fb can be used to constraint the parameters (such as f, m_ϕ, m_{W_H}, and m_{ν_H}) and give the contours between them, as shown in Figs. 4 and 6.

B. The contour of m_{W_H} and m_{ν_H} in the W_H-mediated process

Since the relationships of the parameters in $\gamma\gamma \to \bar{\ell}_i\ell_j$ mediated by the heavy W_H is quite simple, we will use firstly this channel to discuss the dependence of the parameters. Of course, the process $\gamma\gamma \to \bar{\ell}_i\ell_j$ should receive contributions from both the heavy gauge bosons and the charged scalars, and we will discuss this later.

To find the influence of the center-of-mass energy, in Fig. 3 we plot how the cross section changes as $\sqrt{S}$ increases, and the results are as expected. We can see that the production rates of the three channels are almost in the same order, and the trend of every channel is almost flat, so in our following discussion we will take $\sqrt{S} = 200$ GeV and neglect the minor difference induced by it.

From Fig. 3, we also see that the three curves in our precision range are almost the same (at least of the same order), so in the following we will only consider one process (for example, $\bar{\mu}e + \bar{e}\mu$ production).

In Fig. 3 we show the contour of m_{W_H} and m_{ν_H}, where W_H is taken between 200 and 1000 GeV; however, in the actual case we should have a larger m_{W_h} (e.g., larger than 1000 GeV) so that we can conclude that if the 10^{-2} fb limit is assumed, the possibility for m_{W_H} and m_{ν_H} to survive together is quite small.

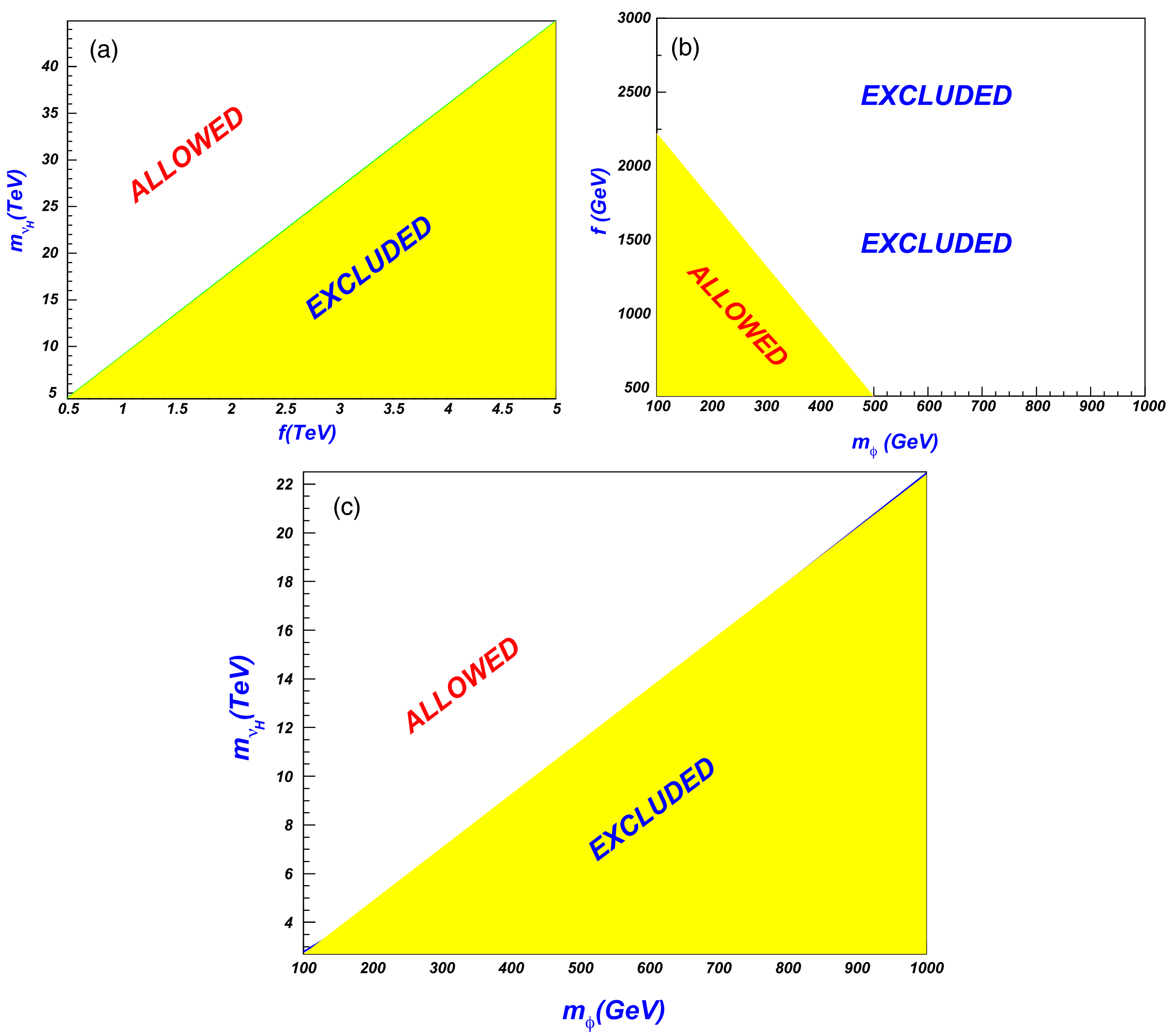

FIG. 6. The contours of f and m_{ν_H} (a), m_ϕ and f (b), and m_ϕ and m_{ν_H} (c).

C. The contributions from f, m_ϕ, m_{ν_H}, and m_{W_H}

The VEVs f and $\hat{f}$ of the two Higgses H and $\hat{H}$, respectively, are taken as $500 \le f \le 5000$ and $\hat{f} = 10f$ in this work [8]. The main parameters involved are m_{W_H}, m_ϕ, m_{ν_H}, the Higgs VEV f, and the mixing matrix V_H, which will be emphatically discussed.

We show in Fig. 5 the dependence of f, the scalar mass m_ϕ, the heavy neutrino mass m_{ν_H}, and the heavy charged boson mass m_{W_H}. We also see from Fig. 5 that the dependences on f, m_{ν_H}, m_ϕ, and m_{W_H} are large enough to be detectable in some parameter space, for the 10^{-2} limit, with the requirements that $f < 1400$ GeV, $m_{\nu_H} > 6000$ GeV, and looser requirements for m_ϕ and m_{W_H}.

We notice in Figs. 5(a) and 5(b) that the f and m_{ν_H} dependences have opposite influences on the production rates—i.e., the cross section increases as m_{ν_H} increases, or as f decreases—which can be understood from Eq. (7), where we see that the coupling of $\phi\bar{l}\nu_H$ is proportional to m_{ν_H} and inversely proportional to f.

The production rates with m_ϕ in Fig. 5(c) are large, and the total range of the vertical axis is not too wide (0.009–0.018 fb), which provides the possibility to measure the scalar mass.

From Fig. 5(d) we can see that the m_{W_H} dependence seems quite large; however, the contributions of m_{W_H} and f are not related to each other, since the couplings of $W_H\bar{l}\nu_H$ in Eq. (8) do not comprise the breaking parameter f. Thus, in Fig. 5(d) the curve of the cross section as a function of m_{W_H} is flat, especially when m_{W_H} becomes large, which is because in the total production the scalar contribution dominates so that the change of the heavy gauge boson mass cannot affect the production order.

Since in Fig. 5 the dependences on f, the scalar mass m_H, and the heavy neutrino mass m_{ν_H} are large, Figs. 6(c) show the contours of m_{ν_H} vs f, f vs m_H, and m_{ν_H} vs m_H, respectively.

In Figs. 6(a) and 6(c) we can see that the two contours have similar trends with regards to m_{ν_H}. As m_{ν_H} increases the cross section will increase as well, so a large m_{ν_H} is favored. We also see in Fig. 6 that in our discussion, if $f > 1000$ GeV, in order for the rates to be detectable, m_{ν_H} must be larger than 8190 GeV, while the scalar mass should be smaller than 300 GeV.

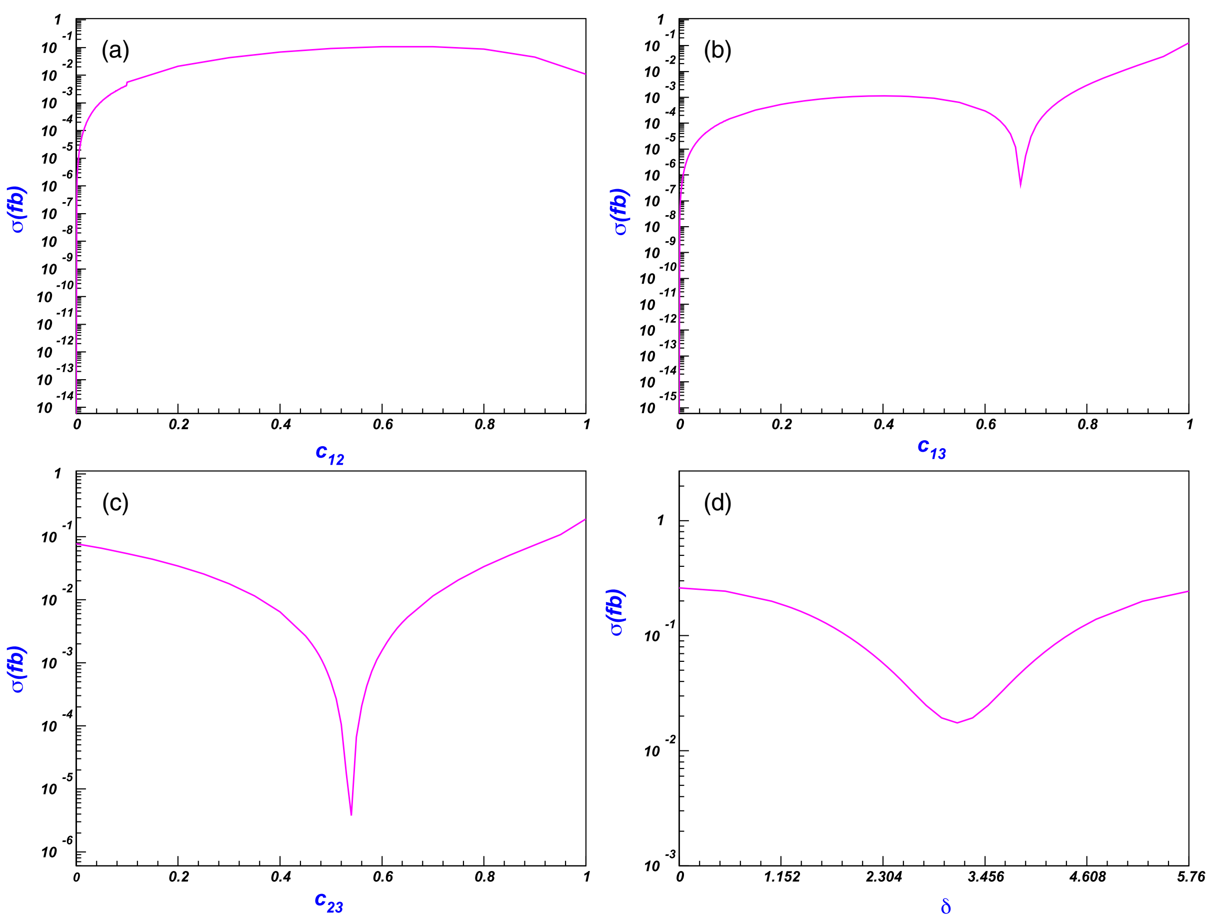

FIG. 7. The production rate as a function of c_{12}, c_{13}, c_{23}, and δ.

In Fig. 6(b) we see the contour between m_ϕ and f; the surviving space is quite small, which is understandable since the largest contribution comes from the mass of the heavy neutrino. We take $m_{\nu_H} = 1000$ GeV in Fig. 6(b), which is not enough to obtain a big production rate, so to arrive at the required cross sections f or m_ϕ should not be too large, which limits them to a small possible space.

From Figs. 6(c), we see that the right-handed neutrino mass provides the largest contribution to the cross section, so this process may serve as a severe constraint on the mass of the heavy neutrino.

Although we have discussed the dependences on m_{W_H}, f, m_ϕ, and m_{ν_H} (see Figs. 4, 3, 5, and 6), we have not considered changing generation mixings, since we have fixed them as the lepton mixing parameters [as in Eq. (19)]. In Fig. 7 we free them and plot the dependence of these mixing parameters. We find that although the cross sections vary large in some ranges, overall they are gradual, especially the curve in Fig. 7(d).

In Figs. 7(a) and 7(b), there are sharp points when $c_{12} = 0$ or $c_{13} = 0$; the reason for this can be found in the expression for the mixing matrix in Eq. (18), in which the elements V_{12} and V_{13} are proportional to s_{12} and s_{13}, respectively. When $c_{12} = 0$ or $c_{13} = 0$, $s_{12} = 1$ or $s_{13} = 1$ contribute quite large.

V. CONCLUSION

We have studied charged scalar- and gauge-boson-mediated lepton-flavor-changing production of $\bar{\ell}_i \ell_j$ $(i \neq j)$ via $\gamma\gamma$ collisions at the ILC. We found that in a certain parameter space, the production rates of $\gamma\gamma \to \bar{\ell}_i \ell_j$ $(i \neq j)$ may arrive at 10^{-2} fb, which means that we may have several events each year for the designed luminosity of about 345 fb^{-1}/year at the ILC. Due to the negligible observation of such $\bar{\ell}_i \ell_j$ events in the SM, it would be a detection of the left-right twin Higgs models in the lepton sector.

More importantly, if we cannot detect the process, this may strictly constrain the parameters. For example, if the process is undetectable, we can impose an upper limit on the Higgs breaking scale f. We can see from Fig. 5(a) that in order to arrive at a cross section of 10^{-2} fb, f should be less than 1.4 TeV in the given parameter space.

Moreover, since the LFV couplings are closely related to the heavy neutrino masses, we may obtain interesting information for the heavy neutrino masses if we could see any signature of the LFV processes. In Fig. 5(b), to arrive at a cross section of 10^{-2} fb, the heavy neutrino mass m_{ν_H} should be larger than 6 TeV in the given parameter space.

Therefore, these LFV processes may serve as a sensitive probe of and a strict constraint on this kind of new physics models.

ACKNOWLEDGMENTS

This work was supported by Excellent Youth Foundation of Zhengzhou University under Grants No. 1421317053 and 1421317054, and the Natural Science Foundation of China under Grant No. 11605110.

[1] See, for example, M. C. Gonzalez-Garcia and Y. Nir, Rev. Mod. Phys. **75**, 345 (2003); V. Barger, D. Marfatia, and K. Whisnant, Int. J. Mod. Phys E **12**, 569 (2003); A. Y. Smimov, arXiv:hep-ph/0402264; M. C. Gonzalez-Garcia and M. Maltoni, Phys. Rep. **460**, 1 (2008).
[2] Y. A. Golfand and E. P. Likhtman, JETP Lett. **13**, 323 (1971) [Pis'ma Zh. Eksp. Teor. Fiz. **13**, 452 (1971)]; D. V. Volkov and V. P. Akulov, Phys. Lett. **46B**, 109 (1973); J. Wess and B. Zumino, Nucl. Phys. **B70**, 39 (1974).
[3] C. T. Hill, Phys. Lett. B **345**, 483 (1995); K. Lane and E. Eichten, Phys. Lett. B **352**, 382 (1995); K. Lane, Phys. Lett. B **433**, 96 (1998); G. Cvetic, Rev. Mod. Phys. **71**, 513 (1999); C. T. Hill and E. H. Simmons, Phys. Rep. **381**, 235 (2003).
[4] N. Arkani-Hamed, A. G. Cohen, T. Gregoire, E. Katz, A. E. Nelson, and J. G. Wacker, J. High Energy Phys. 08 (2002) 021; J. G. Wacker, Nucl. Phys. B, Proc. Suppl. **117**, 728 (2003); M. Schmaltz, Nucl. Phys. B, Proc. Suppl. **117**, 40 (2003); M. Schmaltz and D. Tucker-Smith, Annu. Rev. Nucl. Part. Sci. **55**, 229 (2005).
[5] J. Schechter and J. W. F. Valle, Phys. Rev. D **22**, 2227 (1980); T. P. Cheng and L. F. Li, Phys. Rev. D **22**, 2860 (1980).
[6] Z. Chacko, H.-S. Goh, and R. Harnik, Phys. Rev. Lett. **96**, 231802 (2006); Z. Chacko, Y. Nomura, M. Papucci, and G. Perez, J. High Energy Phys. 01 (2006) 126; Z. Chacko, H. Goh, and R. Harnik, J. High Energy Phys. 01 (2006) 108.
[7] See http://ilcdoc.linearcollider.org/record/6321/files/ILC_RDR_Volume_1-Executive_Summary.pdf?version=4; H. Braun *et al.* (CLIC Study Team Collaboration), Report Nos. CLIC-NOTE-764, CLIC 2008 parameters, http://www.clic-study.org.
[8] A. Abada and I. Hidalgo, Phys. Rev. D **77**, 113013 (2008).
[9] B. Badelek *et al.*, Int. J. Mod. Phys. A **19**, 5097 (2004); J. Gronberg, arXiv:1203.0031; R. Nisius, arXiv:hep-ex/9811024; A. Rosca, Eur. Phys. J. C **33**, s1044 (2004).
[10] K. J. Abraham, K. Whisnant, and B.-L. Young, Phys. Lett. B **419**, 381 (1998).
[11] J.-j. Cao, G.-l. Liu, and J. M. Yang, Eur. Phys. J. C **41**, 381 (2005).

[12] H.-S. Goh and S. Su, Phys. Rev. D **75**, 075010 (2007).

[13] I. F. Ginzburg, G. L. Kotkin, S. L. Panfil, V. G. Serbo, and V. I. Telnov, Nucl. Instrum. Methods Phys. Res., Sect. A **219**, 5 (1984); V. I. Telnov, Nucl. Instrum. Methods Phys. Res., Sect. A **294**, 72 (1990).

[14] J. J. Cao, G. Eilam, M. Frank, K. Hikasa, G. L. Liu, I. Turan, and J. M. Yang, Phys. Rev. D **75**, 075021 (2007).

[15] T. P. Cheng and L.-F. Li, *Gauge Theory of Elementary Particle Physics* (Oxford University, New York, 1984).

[16] T. Hahn and M. Perez-Victoria, Comput. Phys. Commun. **118**, 153 (1999); T. Hahn, Proc. Sci., ACAT2010 (**2010**) 078.

[17] C. Patrignani *et al.* (Particle Data Group Collaboration), Chin. Phys. C **40**, 100001 (2016).

[18] M. Acciarri *et al.* (L3 Collaboration), Phys. Lett. B **496**, 34 (2000); LEP Higgs Working Group Collaboration, arXiv: hep-ex/0107031; ALEPH Collaboration, Phys. Lett. B **487**, 253 (2000); T. Plehn, Phys. Rev. D **67**, 014018 (2003); E. L. Berger, T. Han, J. Jiang, and T. Plehn, Phys. Rev. D **71**, 115012 (2005); A. Melfo, M. Nemevsek, F. Nesti, G. Senjanovic, and Y. Zhang, Phys. Rev. D **85**, 055018 (2012).

[19] CMS Collaboration, Phys. Lett. B **770**, 278 (2017).

[20] Z. Maki, M. Nakagawa, and S. Sakata, Prog. Theor. Phys. **28**, 870 (1962).

[21] A. G. Akeroyd, M. Aoki, and H. Sugiyama, Phys. Rev. D **77**, 075010 (2008).

[22] B. T. Cleveland, T. Daily, R. Davis, Jr., J. R. Distel, K. Lande, C. K. Lee, P. S. Wildenhain, and J. Ullman, Astrophys. J. **496**, 505 (1998); W. Hampel *et al.* (GALLEX Collaboration), Phys. Lett. B **447**, 127 (1999); J. N. Abdurashitov *et al.* (SAGE Collaboration), J. Exp. Theor. Phys. **95**, 181 (2002) [Zh. Eksp. Teor. Fiz. **122**, 211 (2002)]; J. Hosaka *et al.* (Super-Kamiokande Collaboration), Phys. Rev. D **73**, 112001 (2006); B. Aharmim *et al.* (SNO Collaboration), Phys. Rev. Lett. **101**, 111301 (2008); C. Arpesella *et al.* (The Borexino Collaboration), Phys. Rev. Lett. **101**, 091302 (2008).

[23] Y. Ashie *et al.* (Super-Kamiokande Collaboration), Phys. Rev. D **71**, 112005 (2005); J. L. Raaf (Super-Kamiokande Collaboration), J. Phys. Conf. Ser. **136**, 022013 (2008).

[24] M. H. Ahn *et al.* (K2K Collaboration), Phys. Rev. D **74**, 072003 (2006); P. Adamson *et al.* (MINOS Collaboration), Phys. Rev. Lett. **101**, 131802 (2008).

[25] F. P. An *et al.* (Daya Bay Collaboration), Chin. Phys. C **37**, 011001 (2013).

[26] S. Luo and Z.-z. Xing, Phys. Rev. D **86**, 073003 (2012); Z.-Z. Xing, Chin. Phys. C **36**, 281 (2012).

[27] M. Cannoni, C. Carimalo, W. Da Silva, and O. Panella, Phys. Rev. D **72**, 115004 (2005); **72**, 119907 (2005).

[28] B. Badelek *et al.*, Int. J. Mod. Phys. A **19**, 5097 (2004).

[29] J. Cao, L. Wu, and J. Yang, Nucl. Phys. **B829**, 370 (2010); S. Yan-Bin, H. Liang, M. Wen-Gan, T. Farshid, Z. Ren-You, and Z. Ya-Jin, J. High Energy Phys. 09 (2004) 043.